# Report on the Search for TeV $\gamma$ emission from 12 Nearby Blazars in the AIROBICC 92/93 Data

J.L. Contreras, A. Moralejo

## 1 The Data Sample

The data sample analyzed in the present work was recorded during the 'run-in' phase of AIROBICC between March 1992 and March 1993 and is hence the same data sample used for the search for gammas from the Crab Nebula. These data were reconstructed in Munich by A. Karle. The number of showers for which the analysis procedure was able to find at least the incident direction of the primary (with the fixed cone fit to AIROBICC data) was about $2.2 \cdot 10^7$ (approximately 60 % of all the recorded events). Then we applied a series of quality cuts to the data, the same we used for the Crab analysis:

1. 'Bad weather' cuts by rejecting the nights in which the median of the light radius was below 50 m, and also those for which the extinction coefficient in the Johnson V band at zenith was above 0.3.
2. 5 meters core-edge cut.
3. $\chi^2$ of the fixed cone fit to AIROBICC time signals $< 2$.
4. AIR. front cone slope between 0-30 mrad, and scint. one between 0-70 mrad.
5. Light radius between 25 and 140 m.
6. Successful NKG-fit to the scintillator data.

Around 20 % of the events fulfilled these conditions. A further cut on $L_{90}$ ($11000 < L_{90} < 25000$ ph/m$^2$) is applied which sets the 'energy window' roughly in the range 50 -100 TeV for gammas (where we may have the best chance to see something from the AGNs). More precisely, according to MC simulation , such a cut in $L_{90}$ corresponds to an energy window between 40 and 100 TeV for $10^o$ gammas and 50 - 125 TeV for $25^o$ gammas (fig 1). Note that these L90 cut values are different from those in the previous version of the report. The present values fit better the interesting energy range.

## 2 Analysis of the data

From the mean number of fired AIROBICC huts (above 30) of the events which satisfy the above conditions we estimate the angular resolution to be about $\sigma_{63} \simeq 0.17^o$ for this reduced sample. We apply the pointing correction estimated by A. Karle: 0.08 $^o$ in declination and $0.076^o/\cos(\delta)$ in right ascension. The uncertainty in this pointing correction is about $0.1^o$, which makes the optimum ON-source search bin to be $1.37 \cdot \sigma_{63}$ (see [3]). The ON source region we use is then a $0.24^o$ radius circle around the pointing-corrected position of

the studied candidate sources. The OFF region has inner and outer radii of 0.5 and 2.4° respectively. The results are shown in table 1. The sum of all sources yields a 1.8 $\sigma$ excess (23.8 excess events over a mean background of 158.3)[5]. See also fig. 5. The overall excess seems to be dominated by the source MS 01166+31 (2.7 $\sigma$). Two more sources show excesses above 1.5 $\sigma$ (fig. 7). We must remark that at lower energies (removing the lower energy cut $L_{90} > 11000$ ph/$m^2$), we see no significant excess (see fig. 4).

In order to test the possibility that the small observed excess is due to photons from the AGNs, we apply a simple gamma/hadron separation procedure, the same we used for the Rome contribution about the Crab. The separation parameter is $\log_{10}(N_s/L_{90})$. In this case we are dealing with larger statistics since we are adding up events from 12 different sources. This allows us to apply a harder cut than that used for the Crab analysis: here we will simply use the cut which maximizes the quality factor ( $Q = f_\gamma/sqrt(f_h)$ ). It corresponds to $\log_{10}(N_s/L_{90}) < 0.2$ .The gamma efficiency is $f_\gamma \simeq 0.5(\pm 0.1)$, and the hadron efficiency is $f_h \simeq 0.1$. The quality factor is only between 1.3 and 1.5 depending on the zenith angle (see 2 and 3). We remark again that for very low statistics, (i.e., in a single source search like the Crab in a similar period) this is not the optimum (in the way that it does not maximize the sensitivity of the search procedure).

After the $\gamma$/hadron separation the excess nearly vanishes (fig. 6). The numbers are also shown (in brackets) in table 1. The ON time $t_{ON}$ for each source is the total time during which the source was 35° within the zenith coinciding with AIROBICC operation after subtraction of dead time.

Just to see exactly where the ON-bin events lie in terms of $\log_{10}(N_s/L_{90})$, we have plotted in fig. 8 the histograms of this parameter both for the ON and the background events (for the same sample plotted on fig. 5). Also the subtraction (after rescaling background) of these two has been plotted to see whether the excess events cluster anywhere or if, on the contrary, their distribution is compatible with background. The latter seems to be the case. The ON bin events $\log_{10}(N_s/L_{90})$ distribution is compatible with the OFF events one with a probability (given by the Kolmogorov test) of 50%. The gaussian fits to the corresponding MC distributions for gammas and hadrons at 10 and 25° can also be seen on fig. 8. Again the ON events appear to be more consistent with background than they are with gammas (see also fig. 9).

Just in case the $\gamma$/hadron separation procedure is, for any reason, not working properly, we can make another kind of test: we remove the 'Bad weather' cuts which were intended only to allow the use of the light density measurement from AIROBICC (in order to use it in the $\gamma$/h separation) and see what comes out with no $\gamma$/h separation. Bad weather does not affect significantly the angular resolution, while removing this cut provides us with larger statistics (35 % more events). The numbers for the 12 AGNs for that sample are then the following: ON: 236, OFF: 213.0. This means that the excess is then slightly lower, 1.6 $\sigma$ instead of larger as one would expect if it was due to a genuine signal.

## 3 Conclusions

We conclude that we see no clear evidence for $\gamma$-emission from the studied sources. In table 2 are the flux upper limits (90% CL) for the generic nearby blazar obtained from the three different samples. To obtain these flux limits we used the following values: the effective area of the array, 170 x 170 $m^2$; the reconstruction efficiency ,about 90%; the fraction of source events within the ON region, which is $> 0.73$, and the $\gamma$-efficiency of the separation cut ($\simeq 0.5$).

Table 1: Events statistics and significances for the 12 AGNs. In brackets, the results after $\gamma$/h separation are shown.

| Source | | z | $N_{Source}$ | $<N_{BG}>$ | S[$\sigma$] | $t_{ON}$(h) |
|---|---|---|---|---|---|---|
| 0116+319 | MS 01166+31 | 0.059 | 28 (2) | 15.9 (0.9) | +2.7 (+1.5) | 87.5 |
| 0430+052 | 3C 120.0 | 0.033 | 11 (0) | 9.6 (1.0) | +0.4 (-1.1) | 76.7 |
| 0802+243 | 3C 192.0 | 0.0599 | 17 (2) | 23.6 (1.8) | -1.4 (-0.1) | 121.5 |
| 1101+384 | Mrk 421 | 0.031 | 21 (0) | 16.1 (1.0) | +1.1 (-1.1) | 99.9 |
| 1214+381 | MS 12143+38 | 0.062 | 18 (1) | 15.2 (1.0) | +0.7 (+0.5) | 89.8 |
| 1514+004 | | 0.05233 | 6 (0) | 2.7 (0.3) | +1.7 (-0.6) | 46.0 |
| 1652+398 | Mrk 501 | 0.03366 | 12 (0) | 14.3 (1.0) | -0.6 (-1.0) | 88.9 |
| 1727+502 | 1Zw 187 | 0.05541 | 10 (0) | 9.1 (0.7) | +0.3 (-0.9) | 82.9 |
| 2200+420 | BL Lac | 0.069 | 11 (0) | 12.7 (0.7) | -0.5 (-0.8) | 81.0 |
| 2201+044 | | 0.028 | 9 (2) | 5.0 (0.6) | +1.6 (+1.9) | 51.3 |
| 4C+37.11 | | 0.055 | 22 (1) | 19.6 (1.2) | +0.5 (-1.2) | 108.8 |
| NGC 315 | | 0.0167 | 17 (1) | 14.5 (0.9) | +0.6 (-1.0) | 85.3 |
| total | | | 182 (9) | 158.3 (11.1) | +1.8 (-0.6) | 1019.5 |

Table 2: Flux upper limits for the generic nearby blazar above 55 TeV.

| Weather cut | $\gamma$/h cut | $N_{Source}$ | $<N_{BG}>$ | $t_{ON}$(h) | $N_{UL}$(90%) | $\Phi_{UL}(cm^{-2}s^{-1})$ |
|---|---|---|---|---|---|---|
| no | no | 236 | 213.0 | 1586.9 | 44.1 | $4.1 \cdot 10^{-14}$ |
| yes | no | 182 | 158.3 | 1019.5 | 42.1 | $6.0 \cdot 10^{-14}$ |
| yes | yes | 9 | 11.1 | 1019.5 | 7.0 | $2.0 \cdot 10^{-14}$ |

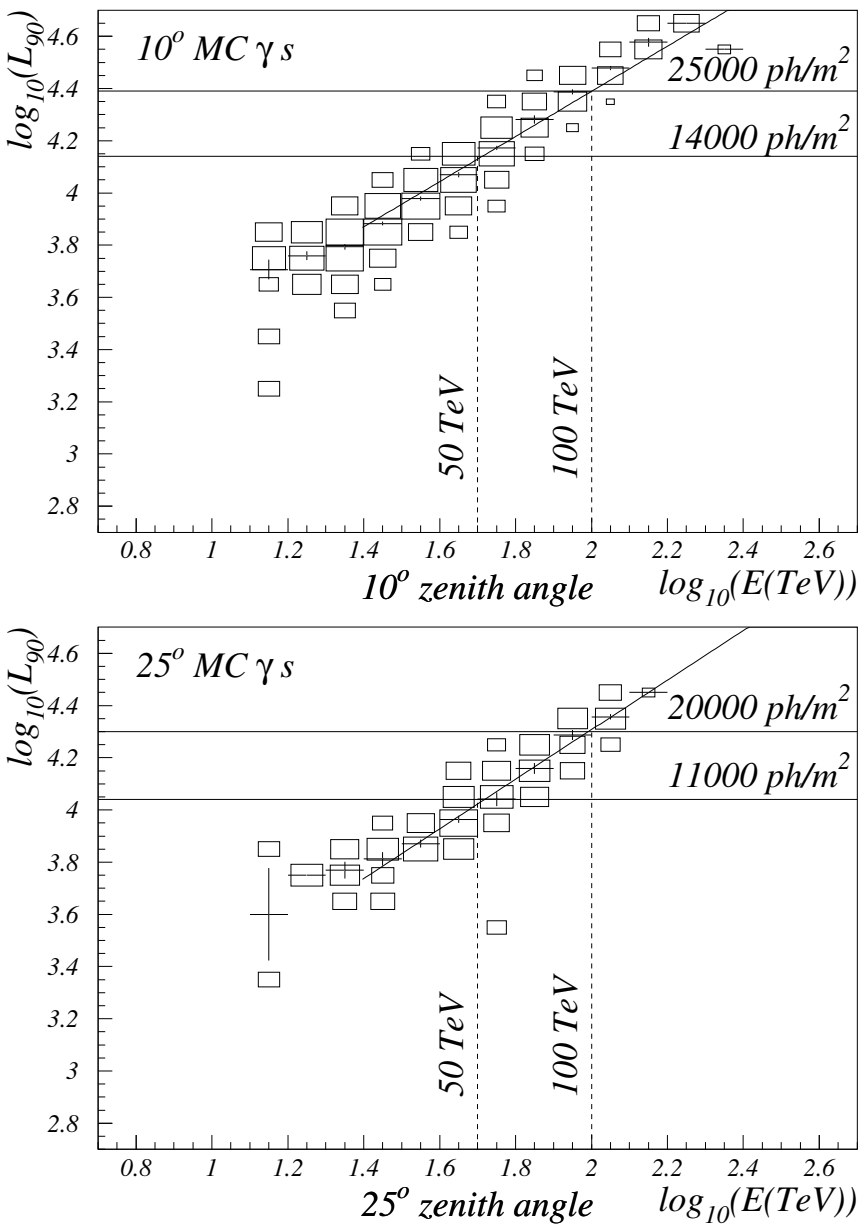


Figure 1: Correlation between $L_{90}$ and the primary energy for MC gammas.

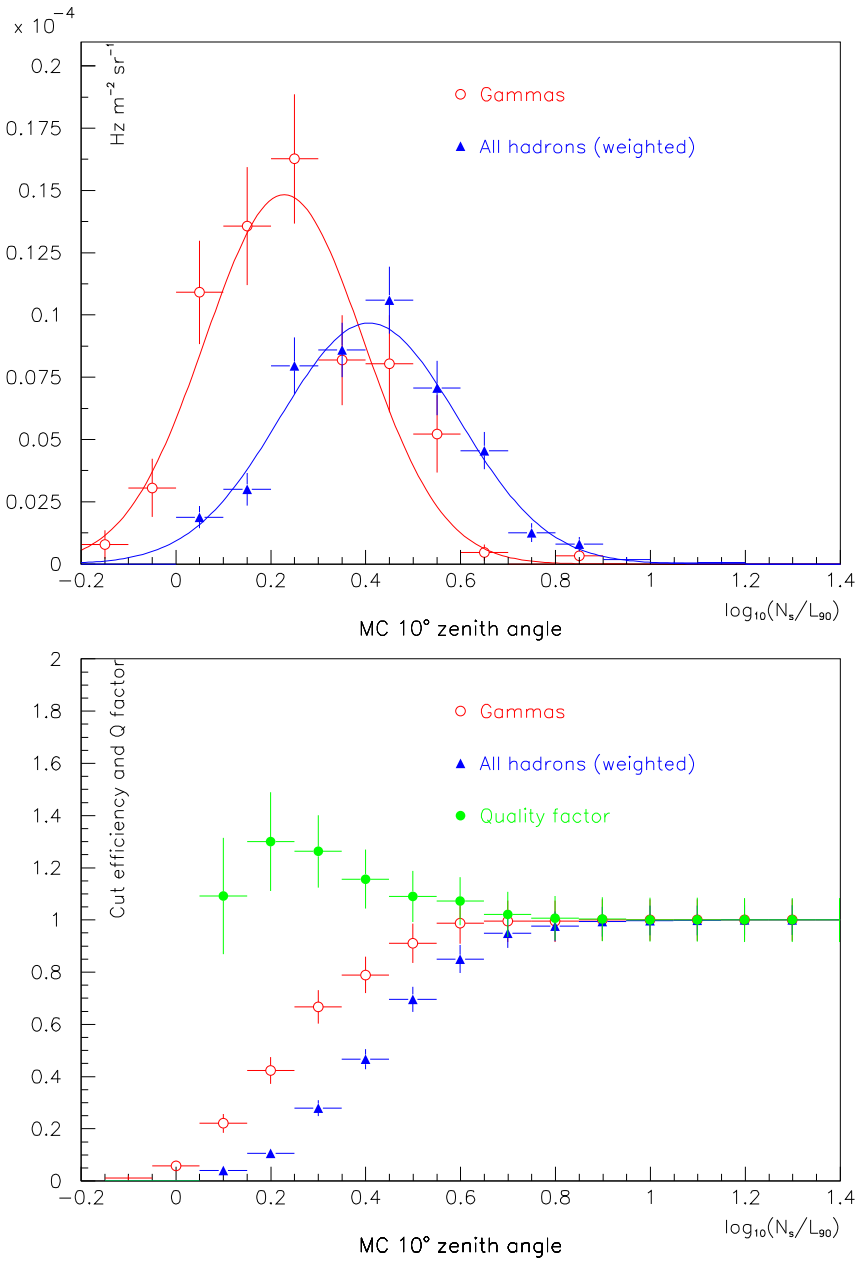


Figure 2: Distribution of the gamma/hadron separation parameter for 10° zenith angle MC events. The efficiencies and the quality factor for different cut values are also shown.

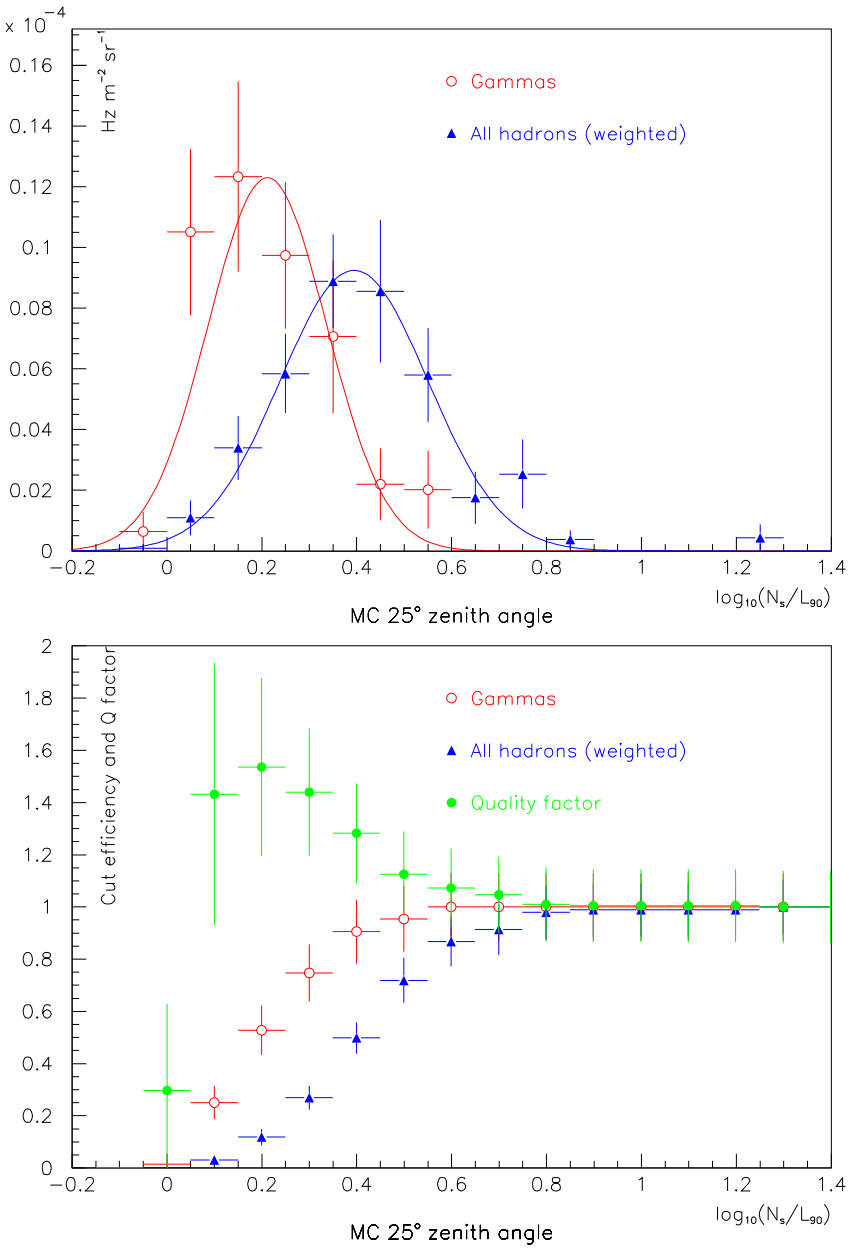


Figure 3: Distribution of the gamma/hadron separation parameter for 25° zenith angle MC events. The efficiencies and the quality factor for different cut values are also shown.

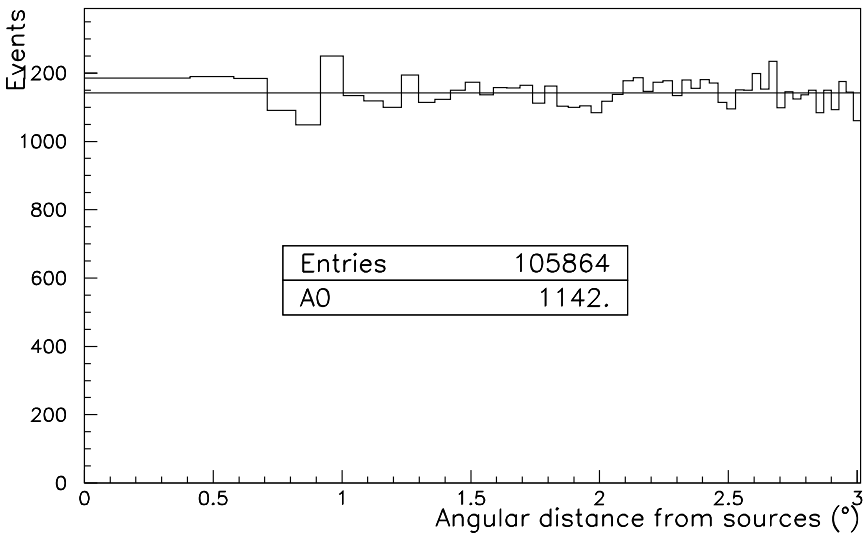


Figure 4: Sum of the 12 AGNs. No 'bad weather' cut, no lower energy cut and no $\gamma$/hadron separation.

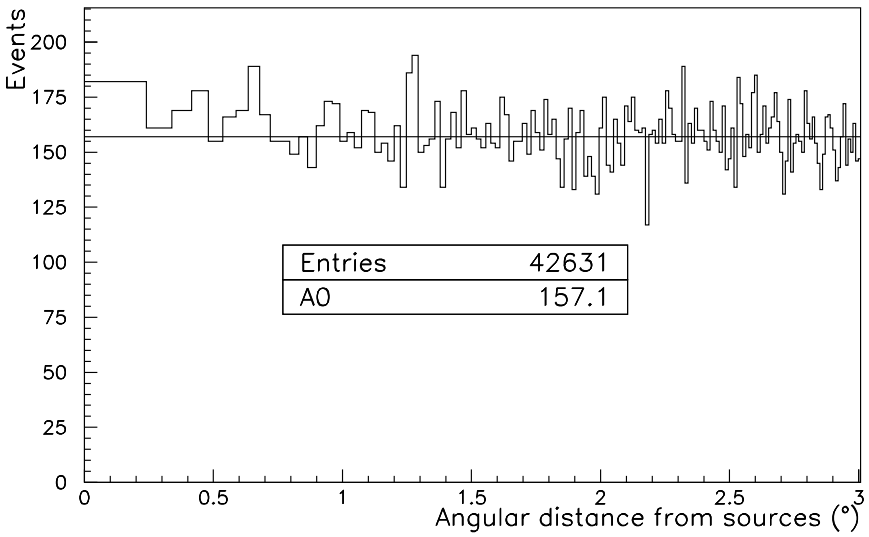


Figure 5: Sum of the 12 AGNs. $11000 < L_{90} < 25000 \quad ph/m^2$. No $\gamma$/hadron separation.

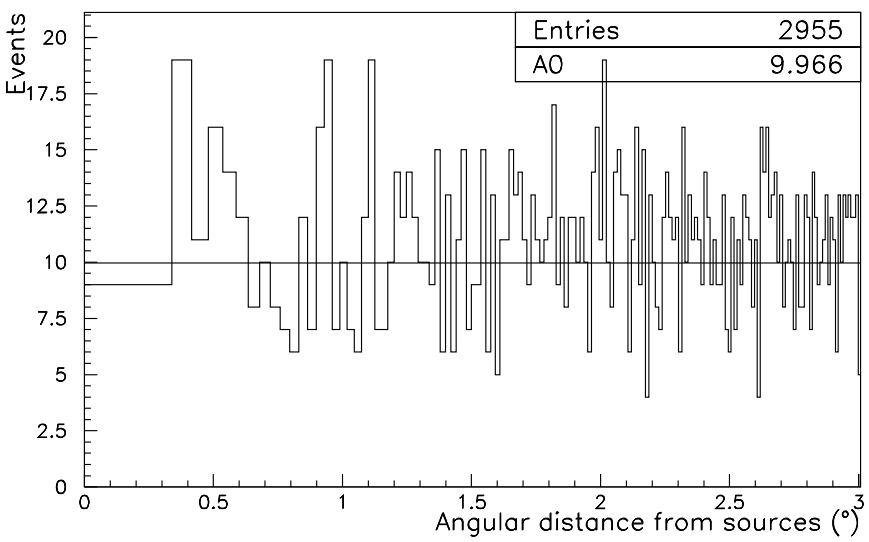


Figure 6: Sum of the 12 AGNs. After $\gamma$/hadron separation.

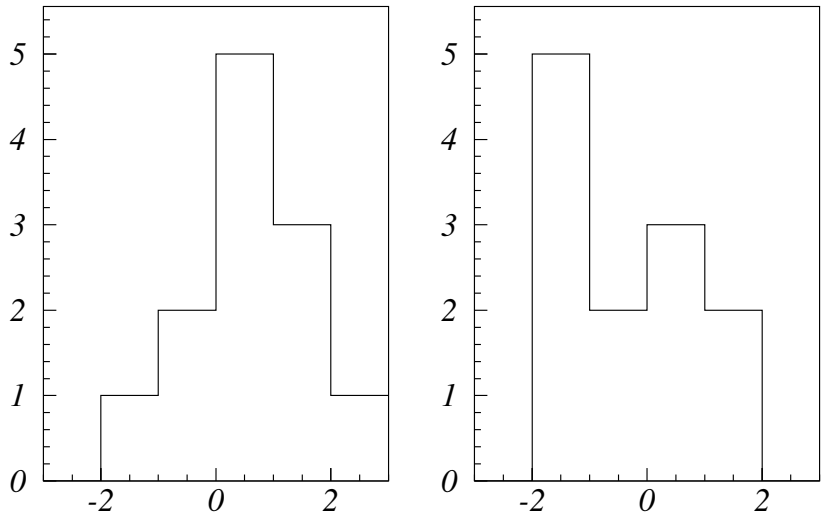

Figure 7: Distribution of significances before (left) and after (right) $\gamma$/hadron cut.

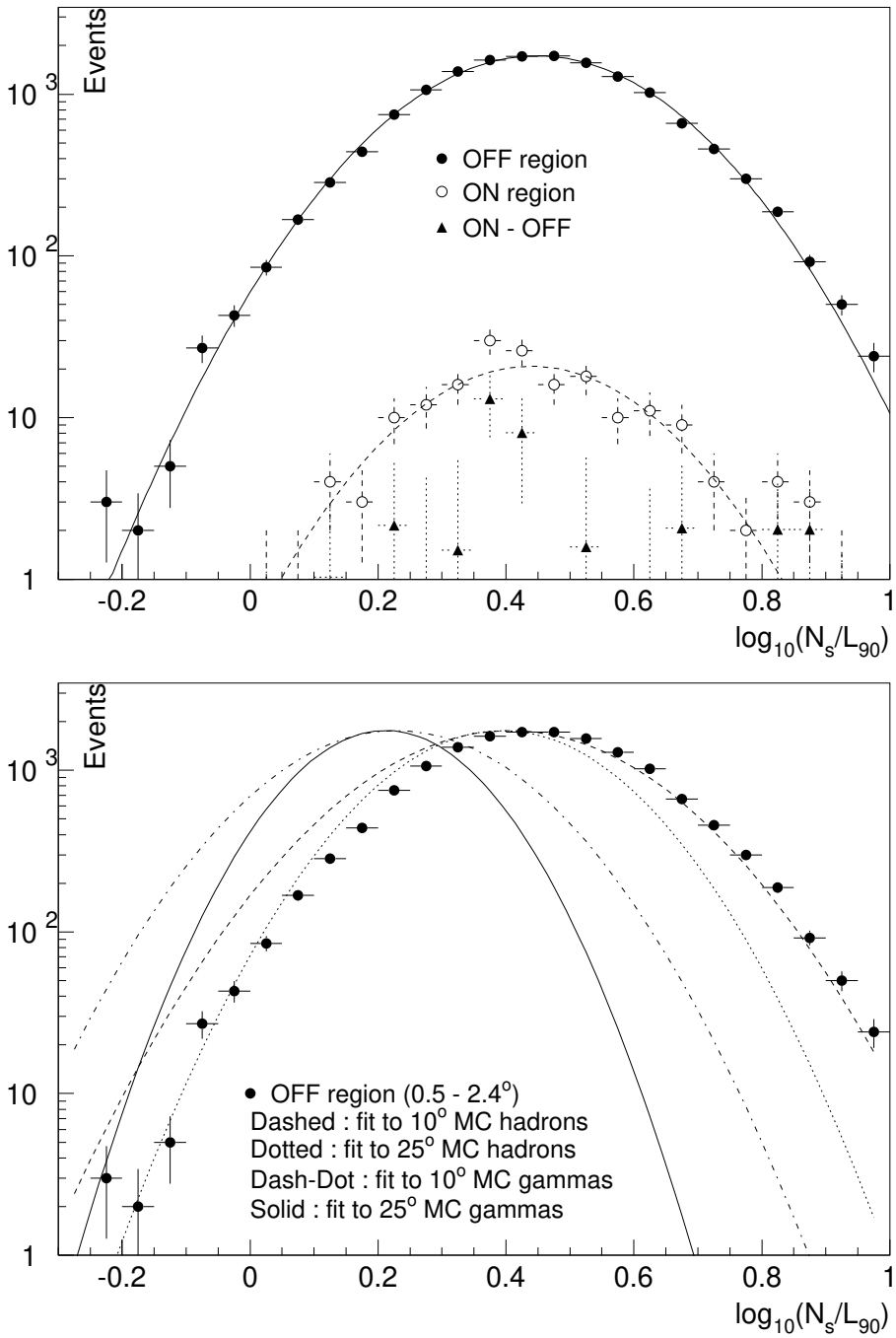


Figure 8: Histograms of the $\gamma$/hadron separation parameter (for the sample showed on fig. 5.

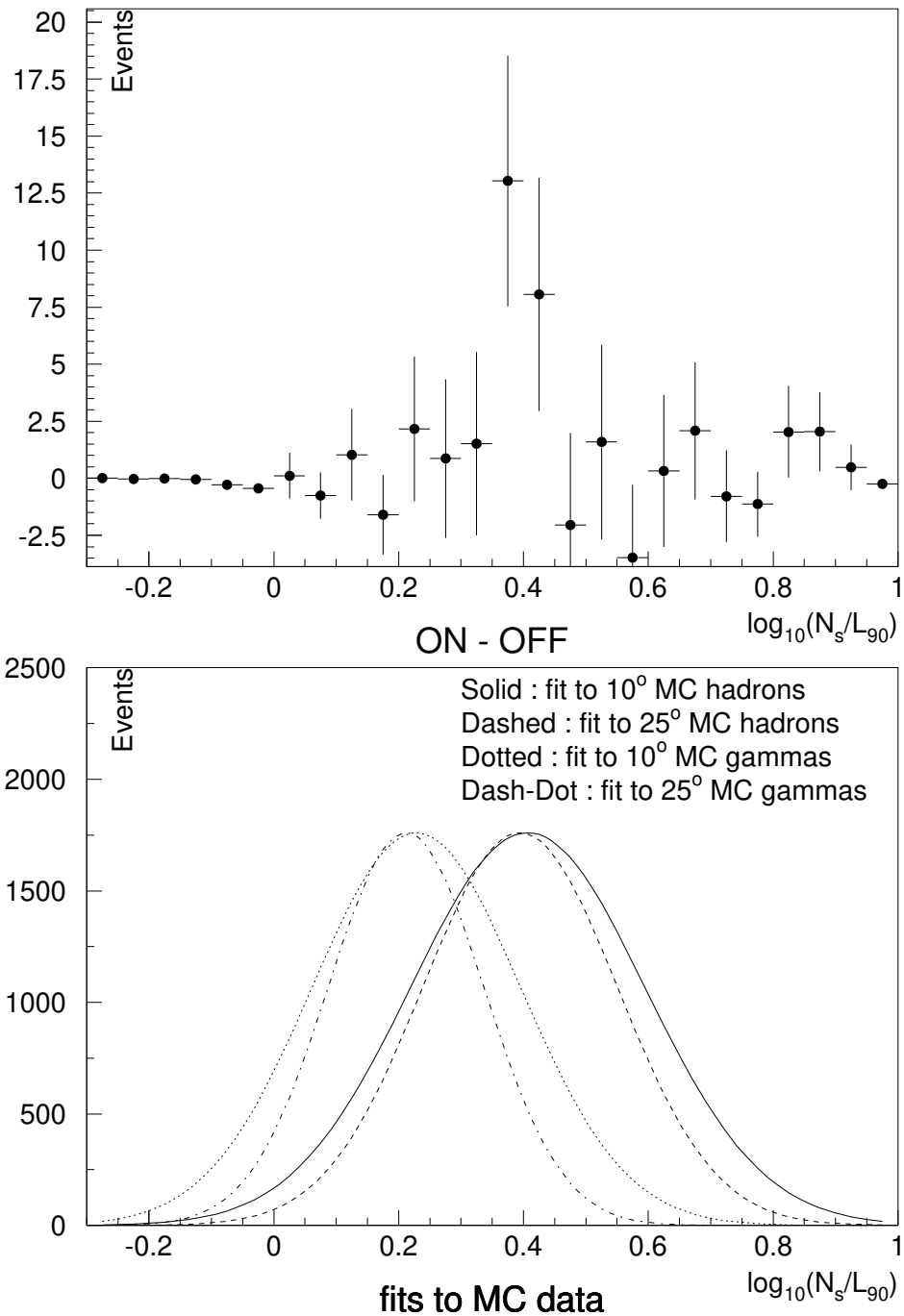


Figure 9: Histograms of the $\gamma$/hadron separation parameter. The real data ON-OFF distribution (top) corresponds to the sample showed on fig. 5.

## References


[1] Karle, A. Thesis, Ludwig-Maximilians-Universität (1994).

[2] Karle A., et al. Phys. Lett. B 347(1995)161.

[3] Karle A., et al. MPI-report MPI/PhE/95-01. Astroparticle Physics 4 (1995) 1-13.

[4] Karle A., et al. MPI-report MPI/PhE/94-29 Submitted to Nucl. Instr. and Meth. A.

[5] Li, Ti-Pei and Ma, Yu-Qian, Astrophysical Journal **272**(1983)317.